



Universiteit  
Leiden  
The Netherlands

## **Inhibiting thyroid activation in aged human explants prevents mechanical induced detrimental signalling by mitigating metabolic processes**

Houtman, E.; Tuerlings, M.; Suchiman, H.E.D.; Lakenberg, N.; Cornelis, F.M.F.; Mei, H.L.; ... ; Meulenbelt, I.

### **Citation**

Houtman, E., Tuerlings, M., Suchiman, H. E. D., Lakenberg, N., Cornelis, F. M. F., Mei, H. L., ... Meulenbelt, I. (2022). Inhibiting thyroid activation in aged human explants prevents mechanical induced detrimental signalling by mitigating metabolic processes. *Rheumatology*. doi:10.1093/rheumatology/keac202

Version: Publisher's Version











License: [Creative Commons CC BY-NC 4.0 license](https://creativecommons.org/licenses/by-nc/4.0/)

Downloaded from: <https://hdl.handle.net/1887/3455609>

**Note:** To cite this publication please use the final published version (if applicable).

## Original article

# Inhibiting thyroid activation in aged human explants prevents mechanical induced detrimental signalling by mitigating metabolic processes

Evelyn Houtman <sup>1</sup>, Margo Tuerlings <sup>1</sup>, H. Eka D. Suchiman<sup>1</sup>, Nico Lakenberg<sup>1</sup>, Frederique M. F. Cornelis <sup>2</sup>, Hailiang Mei <sup>3</sup>, Demiën Broekhuis <sup>4</sup>, Rob G. H. H. Nelissen <sup>4</sup>, Rodrigo Coutinho de Almeida <sup>1</sup>, Yolande F. M. Ramos <sup>1</sup>, Rik J. Lories <sup>2,5</sup>, Luis J. Cruz<sup>6</sup> and Ingrid Meulenbelt <sup>1</sup>

## Abstract

**Objectives.** To investigate whether the deiodinase inhibitor iopanoic acid (IOP) has chondroprotective properties, a mechanical stress induced model of human aged explants was used to test both repeated dosing and slow release of IOP.

**Methods.** Human osteochondral explants subjected to injurious mechanical stress (65%MS) were treated with IOP or IOP encapsulated in poly lactic-co-glycolic acid–polyethylene glycol nanoparticles (NP-IOP). Changes to cartilage integrity and signalling were determined by Mankin scoring of histology, sulphated glycosaminoglycan (sGAG) release and expression levels of catabolic, anabolic and hypertrophic markers. Subsequently, on a subgroup of samples, RNA sequencing was performed on 65%MS ( $n=14$ ) and 65%MS+IOP ( $n=7$ ) treated cartilage to identify IOP's mode of action.

**Results.** Damage from injurious mechanical stress was confirmed by increased cartilage surface damage in the Mankin score, increased sGAG release, and consistent upregulation of catabolic markers and downregulation of anabolic markers. IOP and, though less effective, NP-IOP treatment, reduced *MMP13* and increased *COL2A1* expression. In line with this, IOP and NP-IOP reduced cartilage surface damage induced by 65%MS, while only IOP reduced sGAG release from explants subjected to 65%MS. Lastly, differential expression analysis identified 12 genes in IOP's mode of action to be mainly involved in reducing metabolic processes (*INSIG1*, *DHCR7*, *FADS1* and *ACAT2*) and proliferation and differentiation (*CTGF*, *BMP5* and *FOXM1*).

**Conclusion.** Treatment with the deiodinase inhibitor IOP reduced detrimental changes of injurious mechanical stress. In addition, we identified that its mode of action was likely on metabolic processes, cell proliferation and differentiation.

**Key words:** OA, DIO2, chondrocytes, cartilage, thyroid signalling, iopanoic acid, mechanical stress

## Rheumatology key messages

- Translation of OA risk genes and human disease modelling as an effective route for chondroprotective drug development.
- Mitigation of thyroid signalling by IOP treatment prevents MMP13-induced cartilage damage in mechanically stressed human explants.
- Identification of molecular modes of action highlighted *INSIG1*, *CTGF* and *BMP5* involvement, maintaining chondrocyte resting state.

<sup>1</sup>Molecular Epidemiology, Department of Biomedical Data Sciences, Leiden University Medical Center, Leiden, The Netherlands, <sup>2</sup>Department of Development and Regeneration, Skeletal Biology and Engineering Research Centre, Laboratory of Tissue Homeostasis and Disease, KU Leuven, Leuven, Belgium, <sup>3</sup>Sequencing Analysis Support Core, <sup>4</sup>Department of Orthopaedics, Leiden University Medical Center, Leiden, The Netherlands, <sup>5</sup>Division of Rheumatology, University Hospitals Leuven, Leuven, Belgium and <sup>6</sup>Translational Nanobiomaterials and Imaging (TNI)

Group, Department of Radiology, Leiden University Medical Center, Leiden, the Netherlands

Submitted 20 October 2021; accepted 24 March 2022

Correspondence to: Ingrid Meulenbelt, Molecular Epidemiology, Department of Biomedical Data Sciences Postzone J-11-R, Albinusdreef 2, 2333 ZA Leiden, The Netherlands.  
E-mail: i.meulenbelt@lumc.nl

## Introduction

OA is a prevalent and debilitating age-related disease. It is a progressive disease characterized by cartilage degeneration and osteophyte formation [1]. Given the ageing society with increasing obesity rates, OA is projected to be the most frequent disease in the Dutch population in 2040, affecting 2.3 million people. Due to the fact that there is no effective treatment, except for joint replacement surgery, OA has a considerable social and economic burden on the ageing population.

Chondrocytes reside in healthy articular cartilage in a maturation-arrested state without detectable proliferation and with low metabolic activity [2]. Yet, with an inherently low tissue repair capacity of chondrocytes, the integrity of cartilage tissue is irreversibly affected upon environmental challenges such as injurious mechanical stress [3]. By applying molecular profiling of human OA articular cartilage, it has been consistently shown that activated articular chondrocytes with OA pathophysiology lose their healthy maturation-arrested state and recapitulate an activated growth plate morphology with associated debilitating gene expression [4]. To delineate underlying OA disease aetiology, large-scale genetic studies have been performed and provided further evidence that indeed genes orchestrating the endochondral ossification processes of growth plate chondrocytes could be, among others, a common underlying OA pathway [5]. Basing clinical development on functional data of OA risk genes could have measurable impact on development of effective disease modifying OA drugs given that the presence of genetically supported targets doubles the success rate of a drug in clinical development [6].

An example of such an OA risk gene is *DIO2*, encoding the deiodinase iodothyronine type-2 (D2) [7]. D2 is an enzyme that converts intracellular thyroxine (T4) into triiodothyronine (T3) in specific tissues such as growth plate cartilage. Here, T3 initiates terminal maturation of hypertrophic chondrocytes leading to breakdown and mineralization of cartilage to allow transition to bone [8]. Functional genomic studies have demonstrated that the *DIO2* risk allele rs225014-C has an increased expression relative to the reference allele rs225014-T [9]. Moreover, in human preserved and lesioned OA articular cartilage, upregulated *DIO2* expression has been shown to be a common and consistent phenomenon, particularly relative to healthy cartilage [10]. *In vitro* 3D chondrogenesis with human bone marrow mesenchymal stem cells indicated that overexpression of *DIO2* had a detrimental effect on matrix deposition while iopanoic acid (IOP), a potent inhibitor of deiodinases like D2, had beneficial effects on matrix deposition [11, 12]. In line with this, *Dio2* knockout mice were protected from running-induced joint damage [11]. Transgenic rats with cartilage-specific overexpression of human *DIO2* (hD2Tg) did not show any articular cartilage defects [13]. However, upon increasing the biomechanical burden by applying an injury-induced OA model, hD2Tg rats showed significantly higher levels of cartilage damage

compared with their wild-type littermates. Taken together, it was hypothesized that *DIO2* might confer risk to OA by affecting the propensity of maturation-arrested articular chondrocytes to recuperate growth plate morphology upon environmental challenges such as injurious mechanical stress. Additionally, IOP, a previously approved pharmaceutical agent, was delineated as mitigating this process [14].

The current study aimed to confirm chondroprotective effects of the D2 inhibitor IOP in a previously established *ex vivo* aged human osteochondral explant model in which injurious mechanical stress is applied to inflict OA-like damage [15]. To improve treatment efficacy of the small IOP molecule, we investigated efficiency of IOP encapsulated in poly lactic-co-glycolic acid (PLGA) polyethylene glycol (PEG) nanoparticles (NP-IOP) to establish slow prolonged release. Finally, RNA sequencing was performed to explore the mode of IOP treatment action by addressing transcriptome-wide gene expression changes.

## Methods

### Study design and culture condition

Osteochondral explants were obtained from knee joints included in the Research in Articular Osteoarthritis Cartilage (RAAK) study [16]. The RAAK study has been approved by the medical ethical committee of the Leiden University Medical Center (P08.239/P19.013) and informed consent was obtained from subjects. Osteochondral explants were punched from human OA knee joints and maintained in standard chondrogenic medium as described in [Supplementary Materials and Methods](#), available at *Rheumatology* online. Medium was refreshed every 3–4 days. During mechanical stress, explants resided in phosphate buffered saline (PBS). In total 83 osteochondral explants were obtained from 16 donors for this study and divided over the following treatment groups: control ( $n=30$  explants;  $N=16$  donors), injurious mechanical stress (65%MS;  $n=25$  explants;  $N=16$  donors), injurious mechanical stress treated with IOP (65%MS+IOP;  $n=11$  explants;  $N=6$  donors) and injurious mechanical stress treated with NP-IOP (65%MS+NP-IOP;  $n=17$  explants;  $N=10$  donors). Donor characteristics are summarized in [Supplementary Table S1](#), available at *Rheumatology* online.

### Ethics

Our study complies with the Declaration of Helsinki. Furthermore, the RAAK study has been approved by the medical ethical committee of the Leiden University Medical Center (P08.239/P19.013) and written informed consent was obtained from subjects.

### Injurious mechanical stress model

Six days after extraction, dynamic unconfined compression was applied at a strain of 65% of explant height at a frequency of 1 Hz using the Mach-1 mechanical

testing system (Biomomentum Inc., Laval, QC, Canada) on four subsequent days as described previously (Supplementary Figure S1, available at *Rheumatology* online) [15].

### IOP treatment

Explants were treated with IOP (100  $\mu$ M; Sigma) or 24  $\mu$ l of NP-IOP (70  $\mu$ g IOP/mg nanoparticles; 5 mg nanoparticles/ml PBS) from day 3 onwards (Supplementary Fig. S1, available at *Rheumatology* online). On day 13, cartilage and bone were separated using a scalpel, snap-frozen in liquid nitrogen and stored at  $-80^{\circ}\text{C}$  for RNA isolation. For histology, a part was fixed in 4% formaldehyde. Medium was collected on day 13 and stored at  $-80^{\circ}\text{C}$ . Details on sGAG measurement, histology and nanoparticle characterization can be found in Supplementary Materials and methods, available at *Rheumatology* online.

### RNA isolation, reverse transcription and quantitative real-time PCR

Cartilage RNA was extracted using a Mixer mill 200 (Retsch GmbH, Haan, Germany) and homogenizing in TRIzol reagent (Thermo Fisher Scientific, Waltham, MA, USA). RNA was extracted with chloroform, precipitated with ethanol, and purified using the RNeasy Mini Kit (Qiagen, GmbH, Hilden, Germany); see Supplementary Materials and methods, available at *Rheumatology* online for detailed description. To measure changes in chondrocyte signalling, we measured gene expression levels by RT-qPCR. Primer sequences are listed in Supplementary Table S2, available at *Rheumatology* online. Fold changes (FC) were determined using the  $2^{-\Delta\Delta\text{CT}}$  method, in which cyclic threshold (CT) levels were adjusted for the housekeeping gene *SDHA* ( $-\Delta\text{C}_T$ ) and subsequently for control samples ( $-\Delta\Delta\text{C}_T$ ). A  $\text{FC} > 1$  represents an upregulation, while  $\text{FC} < 1$  represents a downregulation.

### RNA sequencing

Paired-end  $2 \times 150$  base pair RNA sequencing (Illumina TruSeq mRNA Library Prep Kit, Illumina HiSeq X Ten; Illumina, Inc., San Diego, CA, USA) was performed. Strand-specific RNA sequencing libraries were generated, which yielded on average 14 million reads per sample. Data from the Illumina platform were analysed with an in-house pipeline as previously described [4]; see Supplementary Materials and methods, available at *Rheumatology* online, for detailed description of alignment, mapping, normalization and quality control. In total, 14 668 protein-coding genes were included in further analyses.

### Differential expression analysis and protein-protein interactions

Differential expression analysis was performed for 65%MS+IOP cartilage compared with 65%MS cartilage obtained from osteochondral explants using DESeq2 R package version 1.24 [17] on 14 668 protein-coding

genes. A general linear model assuming a negative binomial distribution was applied and followed by a Wald test between 65%MS+IOP and 65%MS samples with correction for principal component 1. In all analyses, 65%MS samples were set as reference. To correct for multiple testing, the Benjamini–Hochberg method was used, as indicated by the false discovery rate (FDR) in which a significant cut-off value of 0.05 was used. For protein–protein interactions, analysis was performed using the online tool STRING version 11.0 [18].

### RNA sequencing validation by real-time quantitative PCR

For validation and replication, a total of eight paired samples were selected; 200 ng of RNA was processed into cDNA using the First Strand cDNA Synthesis Kit (Roche Applied Science, Almere, The Netherlands). Real-time qPCR was performed and normalized as described above to determine gene expression of *INSIG1*, *DHCR7*, *FADS1*, *CTGF*, *BMP5* and *FOXM1*.

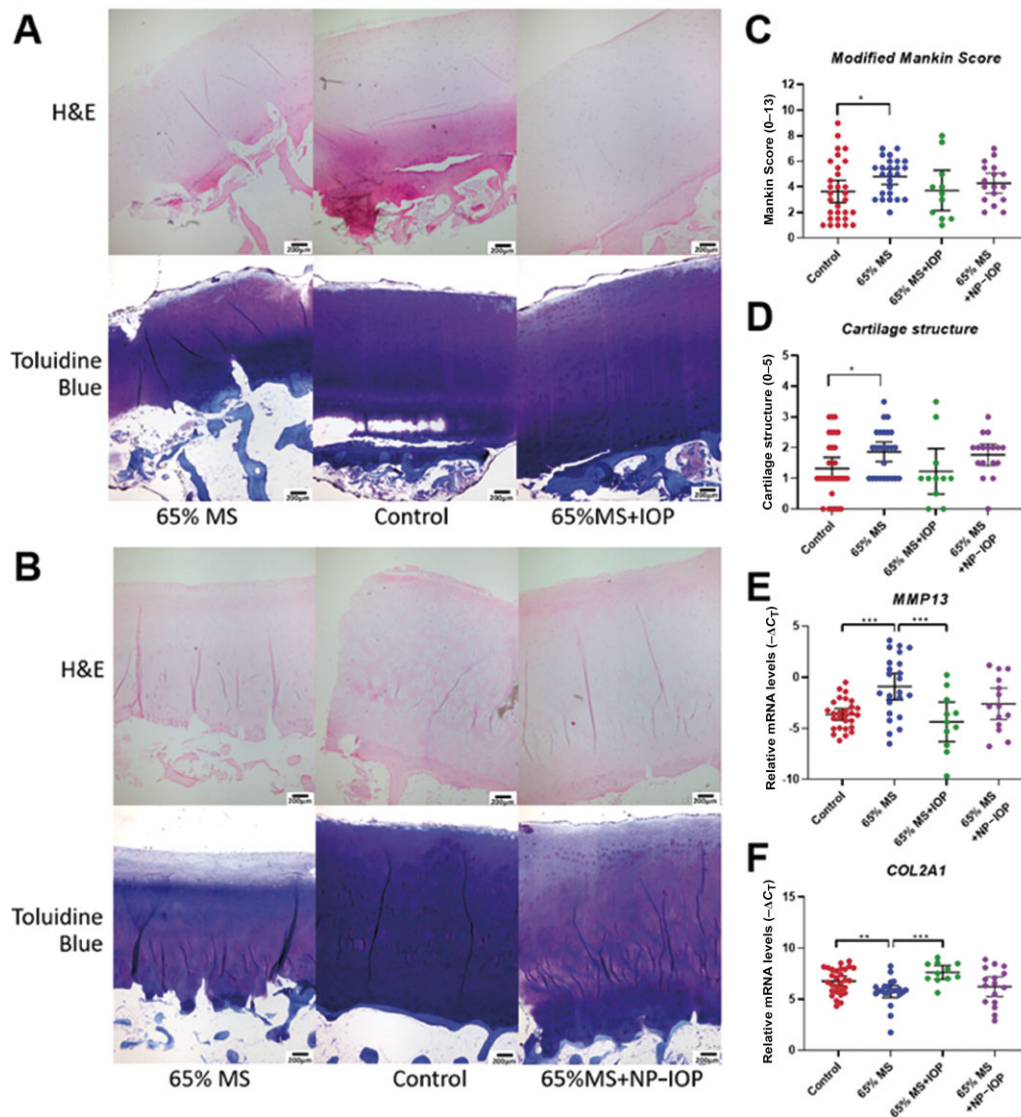
### Statistical analysis

RNA sequencing data analysis was performed in R as described in Supplementary Materials and methods, available at *Rheumatology* online. All other statistical analysis was performed using IBM SPSS Statistics 25 (IBM Corp., Armonk, NY, USA). *P*-values were determined by applying a linear generalized estimating equation (GEE) to effectively adjust for dependencies among donors of the explants by adding a random effect for sample donor as we did not have perfect pairs for each analysis [19]. The following GEE was fitted in which gene expression was the dependent variable and treatment the covariate: Gene expression  $\sim$  Treatment + (1|donor). To determine differences in sGAG concentrations on day 13, another linear GEE model was fitted with sGAG concentration as dependent variable and treatment as covariate: sGAG concentration  $\sim$  Treatment + (1|donor). Differences in Mankin score between groups was determined by applying the following linear GEE model with Mankin score as dependent variable and treatment as covariate: Mankin score  $\sim$  Treatment + (1|donor). Results are described by showing their fold change (FC) or mean (standard error [s.e.]).

## Results

### IOP reduces detrimental chondrocyte signalling induced by 65%MS

First we confirmed that injurious mechanical stress (65%MS) induced detrimental changes to cartilage integrity of control and 65%MS aged human osteochondral explants [15]. Changes in chondrocyte signalling in response to 65%MS were determined by measuring gene expression levels of catabolic (*MMP13*, *ADAMTS5* and *EPAS1*), anabolic (*COL2A1* and *ACAN*) and hypertrophic markers (*COL1A1*, *COL10A1* and *ALPL*). As

**Fig. 1** Mankin score and gene expression of human aged osteochondral explants after treatment with IOP

(A, B) Representative histological images of Toluidine Blue and H&E staining. (C, D) Cartilage damage was assessed by determining the Mankin score (C) with scoring of cartilage structure (D). (E, F) RT-PCR analysis of *MMP13* (E) and *COL2A1* (F). Data are presented as scatter dot plots, with mean and 95% CI, and each circle represents a sample. *P*-values of mean differences between controls and treated explants were estimated by generalized estimating equations (GEE) with expression or Mankin score as dependent variable, treatment as factor and robust variance estimators to account for donor effects. \**P* < 0.05, \*\**P* < 0.01, \*\*\**P* < 0.001. 65%MS: 65% mechanical stress; H&E: haematoxylin and eosin; IOP: iopanoic acid; NP-IOP: nanoparticle-encapsulated IOP.

shown in Fig. 1, non-beneficial chondrocyte responses to 65%MS were particularly marked by increased expression of *MMP13* (FC = 6.61; *P* =  $5.17 \times 10^{-5}$ , Fig. 1E) and *EPAS1* (FC = 1.79; *P* =  $5.49 \times 10^{-6}$ ), and reduced expression of *COL2A1* (FC = 0.49; *P* =  $3.43 \times 10^{-3}$ , Fig. 1F) and *ACAN* (FC = 0.75; *P* =  $1.79 \times 10^{-2}$ ; Table 1).

Next, to investigate if attenuation of thyroid signalling is a promising treatment for OA, osteochondral explants subjected to 65%MS were simultaneously treated with the anti-deiodinase IOP. As shown in Table 1, upon administration of IOP to samples subjected to 65%MS,

catabolic markers *MMP13* (FC = 0.10; *P* =  $1.73 \times 10^{-4}$ ) and *ADAMTS5* (FC = 0.43; *P* =  $2.16 \times 10^{-2}$ ) were down-regulated compared with 65%MS. In addition, expression of the anabolic marker *COL2A1* (FC = 3.58; *P* =  $3.71 \times 10^{-5}$ ; Fig. 1F) was no longer downregulated by 65%MS after IOP treatment. For hypertrophic markers, *COL10A1* (FC = 0.23; *P* =  $1.05 \times 10^{-3}$ ) was significantly downregulated after IOP treatment, while downregulation of *COL1A1* (FC = 0.11; *P* =  $5.29 \times 10^{-2}$ ) and *ALPL* (FC = 0.03; *P* =  $5.71 \times 10^{-2}$ ) did not reach statistical significance. With respect to catabolic marker

**TABLE 1** Summary of outcome parameters in response to the different perturbations

|                        | Control vs 65%MS             |  | 65%MS vs 65%MS+IOP            |                               | 65%MS vs 65%MS+NP-IOP         |                               |
|------------------------|------------------------------|--|-------------------------------|-------------------------------|-------------------------------|-------------------------------|
|                        | FC <sup>a</sup>              | P-value <sup>c</sup>                             | FC <sup>a</sup>               | P-value <sup>c</sup>          | FC <sup>a</sup>               | P-value <sup>c</sup>          |
| <b>Gene expression</b> |                              |  |                               |                               |                               |                               |
| Catabolism             |                              |  |                               |                               |                               |                               |
| <i>MMP13</i>           | 6.44                         | $5.17 \times 10^{-5}$                            | 0.10                          | $1.73 \times 10^{-4}$         | 0.38                          | $9.53 \times 10^{-2}$         |
| <i>ADAMTS5</i>         | 0.90                         | NS   | 0.43                          | $2.16 \times 10^{-2}$         | 0.85                          | NS                            |
| <i>EPAS1</i>           | 1.79                         | $5.49 \times 10^{-6}$                            | 1.32                          | NS                            | 1.21                          | $9.29 \times 10^{-2}$         |
| Anabolism              |                              |  |                               |                               |                               |                               |
| <i>ACAN</i>            | 0.66                         | $1.79 \times 10^{-2}$                            | 1.29                          | NS                            | 1.18                          | NS                            |
| <i>COL2A1</i>          | 0.40                         | $3.43 \times 10^{-3}$                            | 3.58                          | $3.71 \times 10^{-5}$         | 1.68                          | NS                            |
| Hyperthrophy           |                              |  |                               |                               |                               |                               |
| <i>COL1A1</i>          | 1.03                         | NS   | 0.11                          | $5.29 \times 10^{-2}$         | 0.56                          | NS                            |
| <i>COL10A1</i>         | 1.81                         | NS   | 0.23                          | $1.05 \times 10^{-3}$         | 0.93                          | NS                            |
| <i>ALPL</i>            | 1.27                         | NS   | 0.03                          | $5.71 \times 10^{-2}$         | 0.54                          | NS                            |
| <b>Histology</b>       |                              |  |                               |                               |                               |                               |
| Mankin score           | <b>Beta<sup>b</sup></b> 1.15 | <b>P-value<sup>c</sup></b> $2.30 \times 10^{-2}$ | <b>Beta<sup>b</sup></b> -0.83 | <b>P-value<sup>c</sup></b> NS | <b>Beta<sup>b</sup></b> -0.61 | <b>P-value<sup>c</sup></b> NS |
| Cartilage structure    | 0.54                         | $1.90 \times 10^{-2}$                            | -0.48                         | NS                            | -0.16                         | NS                            |
| Cellularity            | 0.25                         | NS   | 0.12                          | NS                            | -0.21                         | NS                            |
| Toluidine blue         | 0.34                         | NS   | -0.42                         | NS                            | -0.21                         | NS                            |
| Tidemark integrity     | 0.14                         | NS   | -0.14                         | NS                            | -0.17                         | NS                            |
| sGAG                   |                              |  |                               |                               |                               |                               |
| Medium                 | 33.68                        | $1.58 \times 10^{-2}$                            | -19.81                        | NS                            | -3.94                         | NS                            |

The comparisons outlined in the table are mechanical stress (65%MS) compared with unperturbed controls, injurious mechanical stress treated with IOP (65%MS+IOP) compared with 65%MS and injurious mechanical stress treated with PLGA nanoparticles filled with IOP (65%MS+NP-IOP) compared with 65%MS. <sup>a</sup>FC is determined by the  $2^{-\Delta\Delta CT}$  method and compared with its respective control. <sup>b</sup>Beta is determined by the GEE during modelling. <sup>c</sup>Significance of mean difference in parameters between explant treatment groups were estimated by generalized estimating equation with robust variance estimators to account for donor effects. 65%MS: 65% mechanical stress; FC: fold change; IOP: iopanoic acid; NP-IOP: nanoparticle-encapsulated IOP; NS: not significant; sGAG: sulphated glycosaminoglycans.

*EPAS1*, no restoration or beneficial effects of IOP treatment with 65%MS was observed.

As a proof of concept and to determine whether IOP delivery from NP-IOP is effective, chondrocyte signalling was measured in response to 65%MS now with NP-IOP treatment. Upon administration of NP-IOP, decreased expression of *MMP13* in comparison with 65%MS as control was observed (FC = 0.38;  $P = 9.53 \times 10^{-2}$ ; Fig. 1 and Table 1), albeit less pronounced and not significant. On the other hand, upon comparing the 65%MS+NP-IOP group with unperturbed controls, changes in *MMP13* and *COL2A1* expression were no longer significant (Fig. 1E and F and Supplementary Table S3, available at *Rheumatology* online). For the hypertrophic markers, no changes were measured in cartilage treated with 65%MS+NP-IOP. To conclude, IOP encapsulated in nanoparticles appears to prevent unbeneficial gene expression changes induced by 65%MS, although effectiveness when compared with repeated treatment with free IOP is less pronounced.

#### IOP reduces cartilage integrity changes in aged human osteochondral explant model

Next, we explored whether the gene expression changes translate to changes in the histological Mankin scores. As shown in Fig. 1A and B, an increased Mankin score

among 65%MS explants as compared with controls [4.80 (0.29) vs 3.65 (0.43);  $P = 2.34 \times 10^{-2}$ ; Fig. 1C] confirmed damage. More specifically, increased Mankin score was particularly due to increased cartilage structure damage score [1.86 (0.15) vs 1.32 (0.18);  $P = 1.94 \times 10^{-2}$ ; Fig. 1D]. Upon investigating explants subjected to 65%MS with IOP or NP-IOP, we observed Mankin scores comparable to controls [3.72 (0.71) and 4.29 (0.37); Fig. 1D, Supplementary Table S3, available at *Rheumatology* online]. In line with this, sGAG released from 65%MS osteochondral explants was increased by 49% compared with controls [91.85 (13.00) vs 61.45 (5.11)  $\mu\text{g/ml}$ ;  $P = 1.58 \times 10^{-2}$ ; Table 1]. Whereas after free IOP treatment, 65%MS induced no change in sGAG release in comparison with controls [61.68 (9.13) vs 61.45 (5.11)  $\mu\text{g/ml}$ ; Supplementary Table S3, available at *Rheumatology* online]. NP-IOP treatment did not reduce sGAG release to the medium with 65%MS [95.91 (14.32) vs 61.45 (5.11)  $\mu\text{g/ml}$ ;  $P = 4.07 \times 10^{-2}$ ; Supplementary Table S3, available at *Rheumatology* online].

#### RNA sequencing of IOP treated explants upon applying 65%MS

To investigate the mode of action of IOP on injurious mechanical stress induced changes, genome-wide gene

expression was measured by sequencing RNA of explant cartilage treated with free IOP and 65%MS ( $n_{65\%MS+IOP}=7$ ) and compared them with the 65%MS group as control ( $n_{65\%MS}=14$ ), as such identifying genes that sequester the damaging response upon injurious loading.

Prior to genome wide analysis, we confirmed expression changes of genes previously measure by RT-qPCR in our osteochondral explant model (Table 1). As shown in Supplementary Table S4, available at *Rheumatology* online, RNA sequencing replicated downregulated expression of *MMP13* (FC=0.06;  $P=9.00 \times 10^{-3}$ ) and of hypertrophic markers *COL1A1* (FC=0.02;  $P=4.72 \times 10^{-4}$ ) and *ALPL* (FC=0.01;  $P=3.65 \times 10^{-3}$ ) in 65%MS+IOP cartilage when compared with 65%MS cartilage. For *COL10A1* (FC=0.18;  $P=6.36 \times 10^{-2}$ ) reduced expression was observed in the RNA sequencing, but did not reach statistical significance. Moreover, despite the similar effect sizes of *COL2A1* in RT-qPCR and RNA sequencing, these effects were not significant in the latter.

Next, genome-wide differential expression analysis with 65%MS as control vs 65%MS+IOP was performed, indicating 12 FDR significant differentially expressed genes (DEGs; Table 2). Of these 12 DEGs, five were upregulated while seven were downregulated with absolute fold changes ranging from 2.25 to 7.69. The highest upregulated gene was *INSIG1* (FC=3.25;  $FDR=2.24 \times 10^{-2}$ ), encoding insulin induced gene 1, a protein inhibiting lipogenesis and cell proliferation [20]. The most downregulated gene was *MASP1* (FC=0.13;  $FDR=3.29 \times 10^{-2}$ ), encoding mannan binding lectin serine peptidase 1, a serine protease involved in complement activation [21]. Of interest is also the identification of downregulated genes promoting chondrocyte proliferation and differentiation such as *BMP5* (FC=0.29;  $FDR=3.29 \times 10^{-2}$ ), encoding bone morphogenetic protein 5, and *CTGF* (FC=0.35;  $FDR=2.24 \times 10^{-2}$ ) encoding connective tissue growth factor [22, 23].

Protein–protein interactions of the DEGs were investigated in STRING and showed significantly more interactions than expected by chance ( $P=2.61 \times 10^{-7}$ ), with 7 out of 12 proteins having connections (Fig. 2). Of note is that connected proteins (*INSIG1*, *DHCR7*, *FADS1* and *ACAT2*) consists of those involved in cholesterol biosynthetic processes (GO: 0006695). To conclude, treatment with IOP shows changes in gene expression patterns that suggest a response in metabolic processes (*INSIG1*, *DHCR7*, *FADS1* and *ACAT2*) and reduction of proliferation and differentiation (*CTGF*, *BMP5* and *FOXM1*) in chondrocytes.

#### Comparison between IOP responsive and OA responsive genes

To investigate to what extend the DEGs coincide with OA pathophysiology, we compared DEGs ( $DEG_{IOP}$ ) with previously identified DEGs between preserved and lesioned OA cartilage ( $DEG_{OA}$ ) [4]. Of the 12 DEGs, three were also involved in OA pathophysiology (Table 3).

**TABLE 2** The 12 FDR significantly differentially expressed genes between IOP and 65% mechanically stressed cartilage

| Gene          | FC   | P-value               | FDR <sup>a</sup>      |
|---------------|------|-----------------------|-----------------------|
| <i>INSIG1</i> | 3.25 | $6.12 \times 10^{-6}$ | $2.24 \times 10^{-2}$ |
| <i>DHCR7</i>  | 2.92 | $1.47 \times 10^{-5}$ | $3.28 \times 10^{-2}$ |
| <i>FADS1</i>  | 2.91 | $1.88 \times 10^{-5}$ | $3.28 \times 10^{-2}$ |
| <i>LRP8</i>   | 2.87 | $3.75 \times 10^{-5}$ | $4.58 \times 10^{-2}$ |
| <i>ACAT2</i>  | 2.25 | $1.55 \times 10^{-5}$ | $3.28 \times 10^{-2}$ |
| <i>LTBP2</i>  | 0.43 | $2.01 \times 10^{-5}$ | $3.28 \times 10^{-2}$ |
| <i>CTGF</i>   | 0.35 | $3.78 \times 10^{-6}$ | $2.24 \times 10^{-2}$ |
| <i>BMP5</i>   | 0.29 | $2.47 \times 10^{-5}$ | $3.29 \times 10^{-2}$ |
| <i>LOX</i>    | 0.23 | $4.14 \times 10^{-6}$ | $2.24 \times 10^{-2}$ |
| <i>ADGRV1</i> | 0.21 | $4.66 \times 10^{-6}$ | $2.24 \times 10^{-2}$ |
| <i>FOXM1</i>  | 0.16 | $1.74 \times 10^{-5}$ | $3.28 \times 10^{-2}$ |
| <i>MASP1</i>  | 0.13 | $2.27 \times 10^{-5}$ | $3.29 \times 10^{-2}$ |

<sup>a</sup>To correct for multiple testing, the Benjamini–Hochberg method was applied to *P*-values and reported as the FDR. FC: fold change; FDR: false discovery rate; IOP: iopanoic acid.

Notable are *ADGRV1*, encoding calcium binding transmembrane receptor adhesion g protein-coupled receptor V1, and *FOXM1*, encoding the transcription factor forkhead box protein M1, a known inducer of cell proliferation and key mediator of inflammatory signalling [24], since they mark OA pathophysiology [4] and are being counteracted by IOP treatment (Table 3). *DHCR7*, a vital enzyme for cholesterol and vitamin D production [25], was upregulated in both OA pathophysiology and in response to IOP treatment. In addition, we investigated if any of the here identified DEGs are also seen as OA susceptibility risk genes and identified that for *BMP5* several polymorphisms have been associated with OA [26, 27].

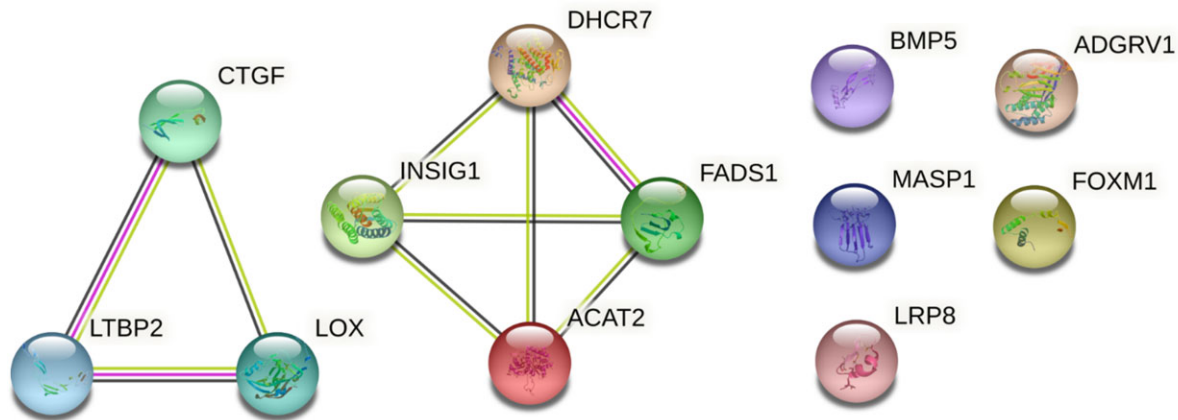
#### Validation of DEGs

For technical validation ( $n=3$  pairs) and biological replication ( $n=5$  pairs) of the DEG identified in this study, RT-qPCR was performed for three upregulated (*INSIG1*, *DHCR7*, *FADS1*) and three downregulated (*CTGF*, *BMP5*, *FOXM1*) genes. For all genes a significant difference was confirmed between 65%MS and 65%MS+IOP treated cartilage (Fig. 3), with the same direction and size of effects, confirming robustness of our RNA sequencing results.

#### Discussion

In the current study we explored possible beneficial effects of inhibiting D2 activity by adding the anti-deiodinase agent IOP to our previously established aged human osteochondral explant model. Herein detrimental effects were initiated by the OA-relevant trigger injurious mechanical stress (65%MS) [15]. To allow further translation of our results we additionally studied effects of

**Fig. 2** Protein–protein interaction network in STRING of proteins encoded by differentially expressed genes



Differentially expressed genes between 65%MS and 65%MS+IOP cartilage of osteochondral explants showing two connected gene groups with high interactions. 65%MS: 65% mechanical stress; IOP: iopanoic acid.

**TABLE 3** Investigation of the 12 FDR significant genes in OA pathophysiology

| Gene          | 65%MS+IOP vs 65%MS |                       |                       | OA pathophysiology <sup>b</sup> |                       |                       |
|---------------|--------------------|-----------------------|-----------------------|---------------------------------|-----------------------|-----------------------|
|               | FC                 | P-value               | FDR <sup>a</sup>      | FC                              | P-value               | FDR <sup>a</sup>      |
| <i>INSIG1</i> | 3.25               | $6.12 \times 10^{-6}$ | $2.24 \times 10^{-2}$ | 1.04                            | NS                    | NS                    |
| <i>DHCR7</i>  | 2.92               | $1.47 \times 10^{-5}$ | $3.28 \times 10^{-2}$ | 1.28                            | $1.21 \times 10^{-3}$ | $1.56 \times 10^{-2}$ |
| <i>FADS1</i>  | 2.91               | $1.88 \times 10^{-5}$ | $3.28 \times 10^{-2}$ | 1.00                            | NS                    | NS                    |
| <i>LRP8</i>   | 2.87               | $3.75 \times 10^{-5}$ | $4.58 \times 10^{-2}$ | 1.15                            | $3.00 \times 10^{-2}$ | NS                    |
| <i>ACAT2</i>  | 2.25               | $1.55 \times 10^{-5}$ | $3.28 \times 10^{-2}$ | 1.19                            | $3.00 \times 10^{-2}$ | NS                    |
| <i>LTBP2</i>  | 0.43               | $2.01 \times 10^{-5}$ | $3.28 \times 10^{-2}$ | 1.06                            | NS                    | NS                    |
| <i>CTGF</i>   | 0.35               | $3.78 \times 10^{-6}$ | $2.24 \times 10^{-2}$ | 1.18                            | $1.00 \times 10^{-2}$ | NS                    |
| <i>BMP5</i>   | 0.29               | $2.47 \times 10^{-5}$ | $3.29 \times 10^{-2}$ | 0.74                            | NS                    | NS                    |
| <i>LOX</i>    | 0.23               | $4.14 \times 10^{-6}$ | $2.24 \times 10^{-2}$ | 1.13                            | NS                    | NS                    |
| <i>ADGRV1</i> | 0.21               | $4.66 \times 10^{-6}$ | $2.24 \times 10^{-2}$ | 1.72                            | $2.87 \times 10^{-3}$ | $2.92 \times 10^{-2}$ |
| <i>FOXM1</i>  | 0.16               | $1.74 \times 10^{-5}$ | $3.28 \times 10^{-2}$ | 1.40                            | $2.31 \times 10^{-3}$ | $2.50 \times 10^{-2}$ |
| <i>MASP1</i>  | 0.13               | $2.27 \times 10^{-5}$ | $3.29 \times 10^{-2}$ | 0.89                            | NS                    | NS                    |

<sup>a</sup>To correct for multiple testing, the Benjamini–Hochberg method was applied to P-values and reported as the FDR. <sup>b</sup>Gene expression changes measured in RNA sequencing data between preserved and lesioned OA articular cartilage, with preserved as reference [4]. 65%MS: 65% mechanical stress; FC: fold change; FDR: false discovery rate; IOP: iopanoic acid; NS: not significant.

prolonged IOP release from nanoparticles. Our results confirmed that treatment with IOP reduced the majority of detrimental 65%MS-induced chondrocyte signalling and even reduced some of its long-term effects on cartilage integrity. Finally, RNA sequencing was performed on 65%MS cartilage with and without IOP treatment, which enable us to identify its mode of action.

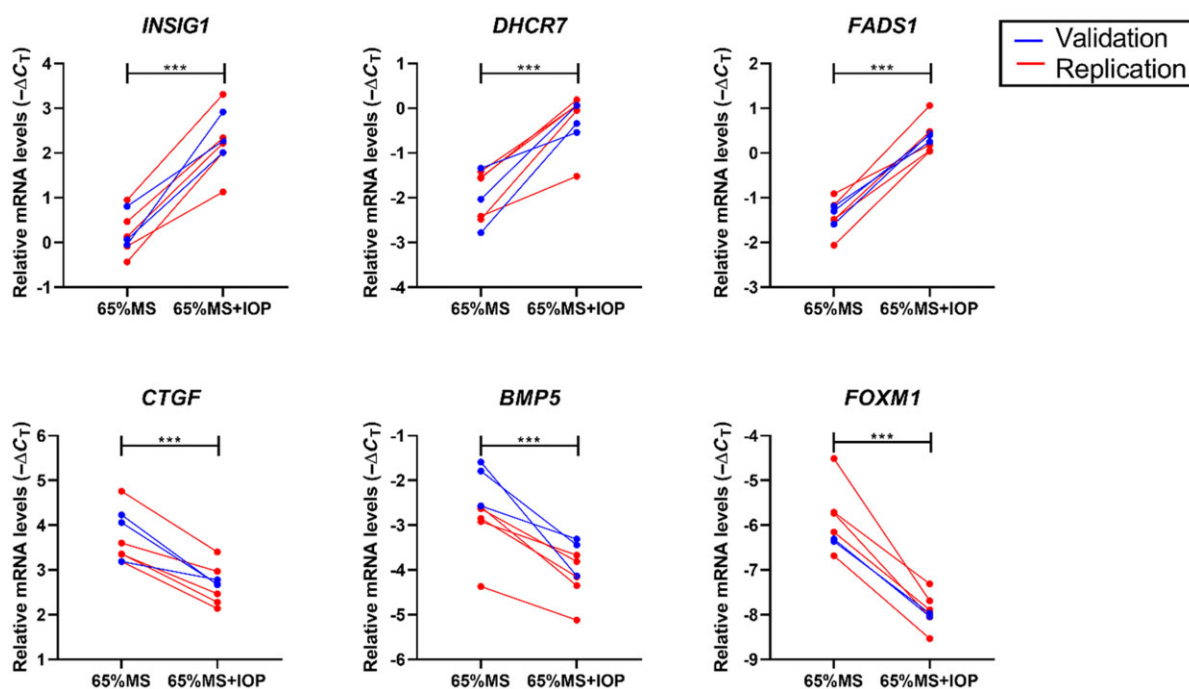
We identified 12 DEGs of which the majority are involved in metabolic processes (e.g. *INSIG1*, *DHCR7*, *FADS2* and *ACAT2*) and cell proliferation and differentiation (e.g. *CTGF*, *BMP5* and *FOXM1*), indicating IOP is reducing metabolic activity of chondrocytes, possibly towards a healthy resting state. This is in line with previous studies showing that adult chondrocytes and the extracellular cartilage matrix benefitted from maintaining

a low metabolic maturation-arrested state, while activation of aged chondrocytes results in proliferation, recapitulation of endochondral ossification and eventually cell death [4, 28].

We here show that treatment with free IOP in the medium efficiently reduced cartilage degradation of human aged osteochondral explants subjected to injurious mechanical stress. These effects were however less pronounced when we administered NP-IOP. A possible explanation for the reduced effectiveness of IOP released from nanoparticles could be that the pharmacological agent is not released in high enough doses to counteract the detrimental induction. This is further exacerbated by the fact that IOP released slowly from the nanoparticles is subject to a half-life of 1–2 days [29],



**Fig. 3** Technical and biological validation of the highest up- and downregulated genes was performed using RT-qPCR



Expression of three upregulated (*INSIG1*, *DHCR7*, *FADS1*) and three downregulated (*CTGF*, *BMP5*, *FOXM1*) genes was validated (blue;  $n = 3$  pairs) and replicated (red;  $n = 5$  pairs) in cartilage samples by RT-qPCR. Figures show connected paired samples and  $-\Delta C_T$  of each independent sample is depicted by black circles in the graphs. Statistical differences between gene expression in 65%MS and IOP treated 65%MS cartilage (65%MS+IOP) was determined with a linear generalized estimation equation with mRNA level as dependent variable.  $***P \leq 0.001$ . 65%MS: 65% mechanical stress; IOP: iopanoic acid; RT-qPCR: reverse transcription-quantitative PCR.

whereas IOP in the medium was refreshed every 3–4 days. On the other hand, the relatively low concentration of  $10 \mu\text{M}$  encapsulated IOP was based on pilot experiments and the underlying thought that NP-IOP is being taken up by chondrocytes (Supplementary Fig 2A, available at *Rheumatology* online), and thus acting locally and more efficiently. In any case, given that NP-IOP appeared less effective, the exact concentration of NP-IOP requires further optimization. Moreover, delivery of the nanoparticles can be further optimized, e.g. by modifying charge of the nanoparticles to increase retention in the synovial cavity or binding to negatively charged sGAGs. Other factors that need to be considered before performing *in vivo* studies are the effects of tissue disease state, synovial fluid and nanoparticle accumulation as these may modify retention, delivery efficiency and drug efficacy.

To investigate the mode of action of IOP, transcriptome-wide differences between cartilage of osteochondral explants subjected to injurious mechanical stress with and without IOP was determined showing 12 FDR significant genes with suggested high protein-protein connectivity (Fig. 2). Notably, these genes appeared to be primarily involved in metabolic processes, such as *INSIG1* ( $\text{FC} = 3.25$ ;  $\text{FDR} = 2.24 \times 10^{-2}$ )

encoding a membrane protein that limits lipogenesis and cell differentiation [20]. Another notable gene in this respect was *BMP5* ( $\text{FC} = 0.29$ ;  $\text{FDR} = 3.29 \times 10^{-2}$ ). *BMP5* is a ligand of the TGF- $\beta$  superfamily involved in activation of SMAD, extracellular signal-regulated kinase and p38 induced gene expression, negatively affecting cartilage homeostasis [30]. On the other hand, *BMP5* silencing reduced OA progression in mice [31]. Together these data suggest that IOP may have reduced detrimental effects of injurious mechanical stress via lowering *BMP5* activation. Of interest is the identification of the transcription factor *FOXM1* ( $\text{FC} = 0.16$ ;  $\text{FDR} = 1.74 \times 10^{-5}$ ), coinciding with genes involved in OA pathophysiology (Table 3) and a key mediator of the inflammatory response inducing OA degeneration [24]. The herein observed downregulation of *FOXM1* suggests that IOP could protect chondrocytes from an inflammatory response upon external stimuli. Finally, because IOP is an inhibitor of thyroid signalling, we compared the 12 DEGs to a consensome meta-analysis of thyroid manipulation studies [32]. Nine (75%) genes were confirmed to be involved in thyroid signalling and among them we identified important genes such as *INSIG1*, *DHCR7*, *FADS1* and *ACAT2* involved in the metabolic process of cholesterol biosynthetic processes

(Supplementary Table S5, available at *Rheumatology* online). To conclude, genome-wide changes resulting from IOP show its ability to reduce the metabolic activity of chondrocytes as observed by the response of genes involved in metabolic processes and cell proliferation and differentiation.

Although the model used in our study is prone to OA pathophysiology, as it consists of physiologically relevant human aged preserved articular cartilage and subchondral bone, the model is inherently subject to heterogeneity. Nonetheless, in general our results were robustly reflected in multiple donors, giving validity to the observed effects. The RNA sequencing was performed in a low number of samples, resulting in limited power to identify DEGs with a lower effect. However, by comparing RT-qPCR results with the RNA sequencing results we show the validity of the results of the RNA sequencing, as observed by similar effect sizes and *P*-values. Altogether, by combining treatment testing of a genetically based (repurposed) drug in an established human aged biomimetic osteochondral explant model of mechanical injury [15, 33], we generated multiple reliable biological replicates on how abrogation of thyroid signalling in cartilage is beneficial for cartilage homeostasis. As such, our approach created reliable data that are highly translatable to the *in vivo* human situation while contributing to the societal need for animal study reduction. In this study we focussed on measuring chondrocyte signalling on the gene expression level since thyroid hormone primarily affects metabolic processes via binding to the thyroid receptor, which regulates downstream gene expression. Additionally, we believe gene expression to be a measurement reflecting detrimental chondrocyte homeostasis prior to any detrimental effects observed in the extracellular matrix.

In this study, we have shown that treatment with the anti-deiodinase IOP reduced detrimental changes induced by injurious mechanical stress. In addition, by performing RNA sequencing we identified that its mode of action mainly encompassed metabolic processes, cell proliferation and differentiation and also important OA-associated genes such as *BMP5*, *CTGF* and *FOXO1*. Since in general a lower metabolism has been shown to be beneficial for chondrocytes, we advocate use of IOP as a potential pharmacological treatment agent for OA.

## Acknowledgements

We thank all the participants of the RAAK study. The LUMC has and is supporting the RAAK study. We thank all the members of our group. We also thank Enrike van der Linden, Robert van der Wal, Peter van Schie, Anika Rabelink-Hoogenstraaten, Shaho Hasan, Maartje Meijer, Daisy Latijnhouwers and Geert Spierenburg for collecting surgical waste material. Data are generated within the scope of the Medical Delta Programs Regenerative Medicine 4D: Generating complex tissues with stem cells and printing technology and Improving Mobility with Technology.

**Funding:** This work was supported by the Dutch Scientific Research council NWO/ZonMW VICI scheme (no. 91816631/528) and the Dutch Arthritis Society/ReumaNederland (15-4-401).

**Disclosure statement:** The authors have declared no competing interests.

## Data availability statement

Data are available on reasonable request. RNA sequencing data underlying this article are available in the European Genome-phenome Archive (EGA) at <https://ega-archive.org/> and can be accessed with EGAS00001006242.

## Supplementary data

Supplementary data are available at *Rheumatology* online.

## References

- 1 Bijlsma JW, Berenbaum F, Lafeber FP. Osteoarthritis: an update with relevance for clinical practice. *Lancet* 2011; 377:2115–26.
- 2 Drissi H, Zuscik M, Rosier R *et al.* Transcriptional regulation of chondrocyte maturation: potential involvement of transcription factors in OA pathogenesis. *Mol Aspects Med* 2005;26:169–79.
- 3 Felson DT. Developments in the clinical understanding of osteoarthritis. *Arthritis Res Ther* 2009;11:203.
- 4 Coutinho de Almeida R, Ramos YFM, Mahfouz A *et al.* RNA sequencing data integration reveals an miRNA interactome of osteoarthritis cartilage. *Ann Rheum Dis* 2019;78:270–7.
- 5 den Hollander W, Ramos YF, Bomer N *et al.* Transcriptional associations of osteoarthritis-mediated loss of epigenetic control in articular cartilage. *Arthritis Rheumatol* 2015;67:2108–16.
- 6 Nelson MR, Tipney H, Painter JL *et al.* The support of human genetic evidence for approved drug indications. *Nat Genet* 2015;47:856–60.
- 7 Meulenbelt I, Min JL, Bos S *et al.* Identification of DIO2 as a new susceptibility locus for symptomatic osteoarthritis. *Hum Mol Genet* 2008;17:1867–75.
- 8 Gereben B, Zavacki AM, Ribich S *et al.* Cellular and molecular basis of deiodinase-regulated thyroid hormone signaling. *Endocr Rev* 2008;29:898–938.
- 9 Bos SD, Bovee JV, Duijnisveld BJ *et al.* Increased type II deiodinase protein in OA-affected cartilage and allelic imbalance of OA risk polymorphism rs225014 at DIO2 in human OA joint tissues. *Ann Rheum Dis* 2012;71: 1254–8.
- 10 Ijiri K, Zerbini LF, Peng H *et al.* Differential expression of GADD45beta in normal and osteoarthritic cartilage: potential role in homeostasis of articular chondrocytes. *Arthritis Rheum* 2008;58:2075–87.
- 11 Bomer N, Cornelis FM, Ramos YF *et al.* The effect of forced exercise on knee joints in Dio2<sup>-/-</sup> mice: type II

- iodothyronine deiodinase-deficient mice are less prone to develop OA-like cartilage damage upon excessive mechanical stress. *Ann Rheum Dis* 2016;75:571–7.
- 12 Bomer N, den Hollander W, Ramos YF *et al.* Underlying molecular mechanisms of DIO2 susceptibility in symptomatic osteoarthritis. *Ann Rheum Dis* 2015;74:1571–9.
  - 13 Nagase H, Nagasawa Y, Tachida Y *et al.* Deiodinase 2 upregulation demonstrated in osteoarthritis patients cartilage causes cartilage destruction in tissue-specific transgenic rats. *Osteoarthritis Cartil* 2013;21:514–23.
  - 14 Tyer NM, Kim TY, Martinez DS. Review of oral cholecystographic agents for the management of hyperthyroidism. *Endocr Pract* 2014;20:1084–92.
  - 15 Houtman E, van Hoolwerff M, Lakenberg N *et al.* Human osteochondral explants: reliable biomimetic models to investigate disease mechanisms and develop personalized treatments for osteoarthritis. *Rheumatol Ther* 2021;8:499–515.
  - 16 Ramos YF, den Hollander W, Bovee JV *et al.* Genes involved in the osteoarthritis process identified through genome wide expression analysis in articular cartilage; the RAAK study. *PLoS One* 2014;9:e103056.
  - 17 Love MI, Huber W, Anders S. Moderated estimation of fold change and dispersion for RNA-seq data with DESeq2. *Genome Biol* 2014;15:550.
  - 18 Szklarczyk D, Gable AL, Lyon D *et al.* STRING v11: protein-protein association networks with increased coverage, supporting functional discovery in genome-wide experimental datasets. *Nucleic Acids Res* 2019;47:D607–13.
  - 19 Diggle P, Liang K-Y, Zeger SL. Analysis of longitudinal data. Oxford: Oxford University Press, 1994, 253.
  - 20 Li J, Takaishi K, Cook W *et al.* Insig-1 “brakes” lipogenesis in adipocytes and inhibits differentiation of preadipocytes. *Proc Natl Acad Sci USA* 2003;100:9476–81.
  - 21 Degn SE, Jensen L, Hansen AG *et al.* Mannan-binding lectin-associated serine protease (MASP)-1 is crucial for lectin pathway activation in human serum, whereas neither MASP-1 nor MASP-3 is required for alternative pathway function. *J Immunol* 2012;189:3957–69.
  - 22 Mailhot G, Yang M, Mason-Savas A *et al.* BMP-5 expression increases during chondrocyte differentiation in vivo and in vitro and promotes proliferation and cartilage matrix synthesis in primary chondrocyte cultures. *J Cell Physiol* 2008;214:56–64.
  - 23 Ivkovic S, Yoon BS, Popoff SN *et al.* Connective tissue growth factor coordinates chondrogenesis and angiogenesis during skeletal development. *Development* 2003;130:2779–91.
  - 24 Zeng RM, Lu XH, Lin J *et al.* Knockdown of FOXM1 attenuates inflammatory response in human osteoarthritis chondrocytes. *Int Immunopharmacol* 2019;68:74–80.
  - 25 Prabhu AV, Luu W, Li D *et al.* DHCR7: a vital enzyme switch between cholesterol and vitamin D production. *Prog Lipid Res* 2016;64:138–51.
  - 26 Southam L, Dowling B, Ferreira A *et al.* Microsatellite association mapping of a primary osteoarthritis susceptibility locus on chromosome 6p12.3-q13. *Arthritis Rheum* 2004;50:3910–4.
  - 27 Tachmazidou I, Hatzikotoulas K, Southam L *et al.*; arcOGEN Consortium. Identification of new therapeutic targets for osteoarthritis through genome-wide analyses of UK Biobank data. *Nat Genet* 2019;51:230–6.
  - 28 Sandell LJ, Aigner T. Articular cartilage and changes in arthritis. An introduction: cell biology of osteoarthritis. *Arthritis Res* 2001;3:107–13.
  - 29 Eason CT, Frampton CM. The plasma pharmacokinetics of iophenoxic and iopanoic acids in goat. *Xenobiotica* 1992;22:185–9.
  - 30 Snelling SJ, Hulley PA, Loughlin J. BMP5 activates multiple signaling pathways and promotes chondrogenic differentiation in the ATDC5 growth plate model. *Growth Factors* 2010;28:268–79.
  - 31 Shao Y, Zhao C, Pan J *et al.* BMP5 silencing inhibits chondrocyte senescence and apoptosis as well as osteoarthritis progression in mice. *Aging (Albany, NY)* 2021;13:9646–64.
  - 32 Ochsner SA, McKenna NJ. No dataset left behind: mechanistic insights into thyroid receptor signaling through transcriptomic consensus meta-analysis. *Thyroid* 2020;30:621–39.
  - 33 Houtman E, Tuerlings M, Riechelmann J *et al.* Elucidating mechano-pathology of osteoarthritis: transcriptome-wide differences in mechanically stressed aged human cartilage explants. *Arthritis Res Ther* 2021;23:215.